Experimental and theoretical studies of the effects of nonuniformities in equilibrium magnetohydrodynamic flows

M. Rosenbaum, S. E. Shamma, and J. F. Louis

Citation: Physics of Fluids **24**, 1032 (1981); doi: 10.1063/1.863494
View online: http://dx.doi.org/10.1063/1.863494
View Table of Contents: http://scitation.aip.org/content/aip/journal/pof1/24/6?ver=pdfcov
Published by the AIP Publishing

Experimental and theoretical studies of the effects of nonuniformities in equilibrium magnetohydrodynamic flows

M. Rosenbaum, S. E. Shamma,[a] and J. F. Louis

Massachusetts Institute of Technology, Cambridge, Massachusetts 02139
(Received 11 June 1980; accepted 11 March 1981)

An experimental study of the effects of thermal and velocity nonuniformities is performed in an equilibrium plasma for a range of Hall coefficients. By introducing equally spaced cold blades in the radial flow of an electrodeless magnetohydrodynamic disk deivce, it is possible to create well-defined two-dimensional wake nonuniformities with strong variations of the plasma properties in the direction normal to the magnetic field and the flow. This type of nonuniformity and orientation theoretically provides the strongest reduction of Hall coefficient and effective conductivity for high values of the Hall coefficient. This degradation which reached more than 50% in some cases, is controlled by both the level of nonuniformities and the value of the ideal Hall coefficient. The former is dependent upon the number of blades (root mean square deviation of the conductivity), and the latter is dependent upon the values of the magnetic field intensities. The results provide basic quantitative information about the effects of conductivity and velocity nonuniformities on the performance of equilibrium magnetohydrodynamic generators over a wide range of Hall coefficients. The theoretical predictions are derived from a detailed two-dimensional electrodynamic analysis and a simplified engineering model based on a generalization of Rosa's layer model. These experiments validate the analytical studies and support the use of the theoretical layer nonuniform models in describing the effect of boundary layers on the performance of linear magnetohydrodynamic devices.

I. INTRODUCTION

The performance of magnetohydrodynamic devices is critically dependent on favorable values of the transport properties of the plasma. It can be seriously influenced by the inhomogeneous distribution of such properties created by the incomplete mixing of seed or fuel, by heat loss mechanisms from the combustor when some percentage of unburned carbon generates hotter and colder gas regions, by wakes of cooled surfaces immersed in the working fluid or by the cooler boundary layers over the walls of magnetohydrodynamic devices.

Very few exact solutions are known for the effective Ohm's law of inhomogeneous plasmas, the best known being that for a layered medium[1] which, for the first time, clearly displayed the strong effect on the Hall coefficient. Other solutions are for two-dimensional symmetric plasmas,[2] as well as the limiting cases[3] of "dilute suspensions" of possibly strong inhomogeneities, and isotropic inhomogeneities with small amplitude.[4] Recent theoretical treatments[5] gave reduction formulae for the effective Ohm's law, valid for high Hall coefficients and strong inhomogeneities, for several types of anisotropic inhomogeneities, including "streamers" in the plane orthogonal to the magnetic field B and plasmas with isotropy in that same plane, but with different degrees of ellipticity along the B direction. The results indicate that the geometry, orientation, intensity, and density of the inhomogeneities are important factors in determining the extent of these effects on the performance and efficiency of magnetohydrodynamic generators.

These analyses[1-7] indicate that plane nonuniformities with strong variations of the plasma properties in the direction normal to the magnetic field and the flow, which provide the strongest degradation effect, would yield a reduction of the effective Hall coefficient as

$$\beta_{\text{eff}} = \frac{\langle\beta\rangle}{\langle\sigma\rangle\langle(1+\beta^2)/\sigma\rangle - \langle\beta\rangle^2} = \frac{\langle\beta\rangle}{G}, \tag{1}$$

where G is Rosa's nonuniformity factor, β is the Hall coefficient, σ is the conductivity, and the averages are in the direction of strong variation of the plasma properties; it indicates the strong influence of the nonuniformities for high β and for high root mean square deviation of the conductivity.

In developing experiments to study the effects of nonuniformities due to thermal and/or velocity deficits or gains in a region of a plasma, it is best to choose favorable conditions and a facility that would isolate the effects of these nonuniformities from other effects. The electrodeless disk geometry, which is a high Hall coefficient device, provides such an environment.

Results from experimental studies are compared with the predictions of two theoretical models derived from a two-dimensional analysis and from a simplified engineering model based on an extension of Rosa's one-dimensional layer theory. These results confirm the theoretical predictions of the effective Hall coefficient and provide basic quantitative information about the effects of conductivity and velocity nonuniformities on the performance of equilibrium magnetohydrodynamic devices over a wide range of Hall coefficients.

II. DESCRIPTION AND RESULTS OF THE EXPERIMENTS

The experiments were performed using the Massachusetts Institute of Technology Shock Tunnel Magnetohydrodynamic Disk Generator.[8] A radial flow magnetohydrodynamic generator was designed and used for these

[a]Permanent address, University of West Florida, Pensacola, Fla. 32504.

 0031-9171/81/061032-08$00.90

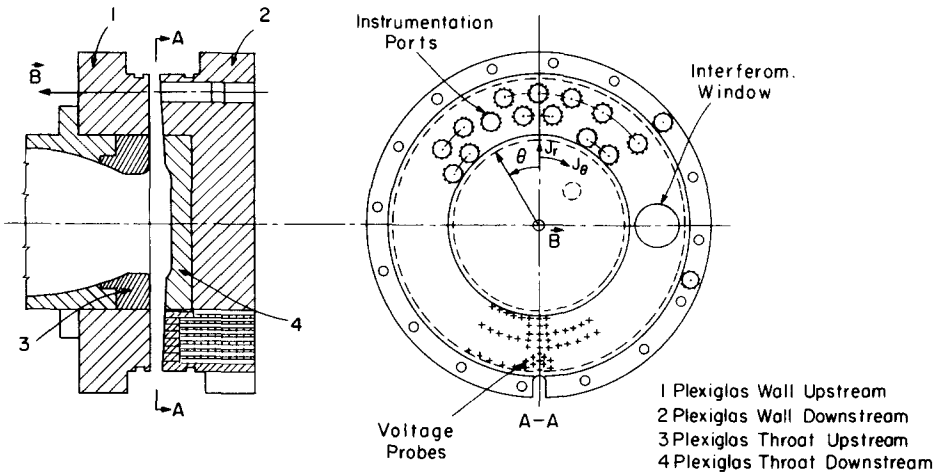

FIG. 1. Radial flow generator.

experiments. Figure 1 is a drawing of the assembly. The downstream wall is convergent with an angle of 3°30′ in order to provide a plasma with nearly constant properties in the test section of the generator.

Up to fifty-one electric field measurements can be made in and out of the thermal wake zones. Instrumentation ports for optical diagnostics (e.g., to determine electron density), and for static pressure measurements are distributed along the disk.

The experiments were carried out in two phases:
(a) determination and characterization of a uniform reference plasma; and
(b) plasma measurements with well-defined wake nonuniformities.

A. Uniform reference plasma experiments

A gas mixture of Ar 80%/CO_2 20%, at room temperature, was used. The higher specific heat ratio of argon, acting like a buffer, provides longer test time, which is a shock tube limitation when only diatomic or triatomic gases are used.

An undisturbed flow was experimentally established, free from background and ionizational nonuniformities which can occur even in molecular gases. Figure 2 shows typical pressure, voltage, and electron density histories. The absence of noticeable fluctuations during the test time supports other evidence, (e.g., $\beta_{eff}=\beta$, as shown in Figs. 15 and 16) that the reference plasma is uniform and in equilibrium.

The chosen test gas provides some degree of simulation of combustion gases. Carbon dioxide at the stagnation conditions dissociates into CO and O_2 in the fraction indicated[9] in Table I, which also reviews the operating conditions used in all cases.

The theoretical plasma profiles were obtained using the two-temperature, one-dimensional model described in Ref. 10 with the inclusion of the different dissociated molecular gas components indicated in Table I. A negligible electron temperature elevation was found for the CO_2 concentration used in the experiment.

Figure 3 shows the predicted and actual pressure, electron density (which is in Saha equilibrium), and conductivity in the disk. The measured conductivity is calculated by using the measured electron density and the effective Hall coefficient, β_{eff}, of the uniform reference plasma. The predicted curves are averages for

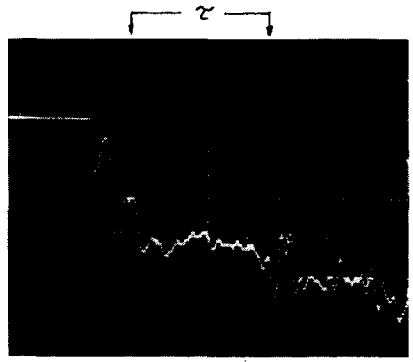

(a) Pressure at r= 11.1 cm

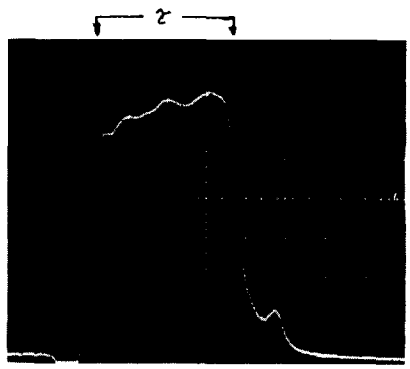

(b) Voltage signal at r= 8.0 cm

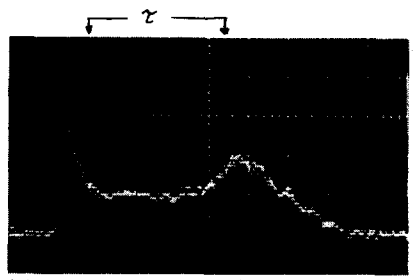

(c) PM Tube signal at r= 10.5 cm

FIG. 2. Typical static pressure, voltage, and PM-tube histories in the disk for the reference flow tests; τ=test time.

TABLE I. Summary of the test conditions.

Mixture of gases (at room temperature)	Ar 80%/CO_2 20%
Relative species concentrations in the stagnation region	Ar 80%; CO_2 12.6%; O_2 3.5%.
Stagnation temperature (°K)	$T_0 = 2850$
Stagnation pressure (atm)	$p_0 = 4.0$
Minimum area A^* (cm^2)	78
r^* (cm)	7.7
h^* (cm)	1.61
Cesium seed fraction	0.25%
Mass flow (kg/sec)	3.0
Test section	
Mach number $\langle M \rangle$	1.40
Test time (msec)	0.7 – 0.8
$\langle \sigma \rangle$ for the uniform reference (mho/m)	30
$\langle \beta \rangle$ for the uniform reference at $B = 3.5$ T	6.5

all applied magnetic field intensities: 1.0, 2.0, 2.6, 3.0, and 3.5 T.

Figure 3 shows that the differences between the theoretical and measured values are within the experimental error; no variations in the pressure and electron density were detected for the different magnetic field intensities due to the low interaction. Figure 4 shows the measured open circuit voltage for the uniform case (no blades case) as a function of the radius for magnetic field intensities of 1.0, 2.0, 3.0, and 3.5 T.

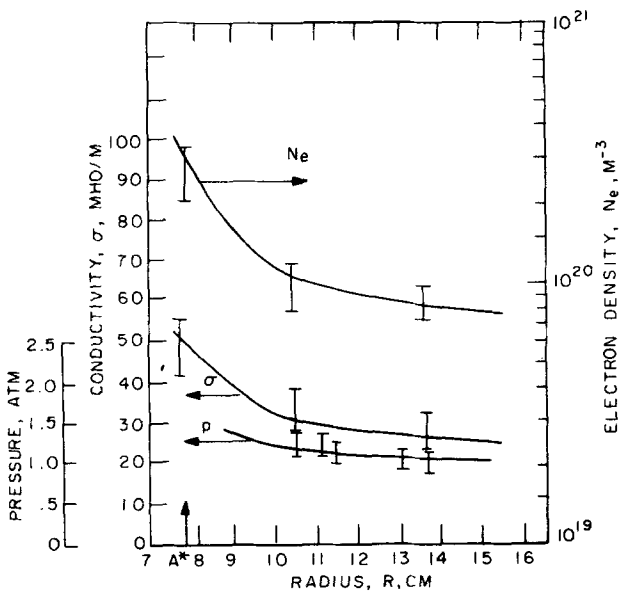

FIG. 3. Measured and calculated electron density, pressure and conductivity in the disk.

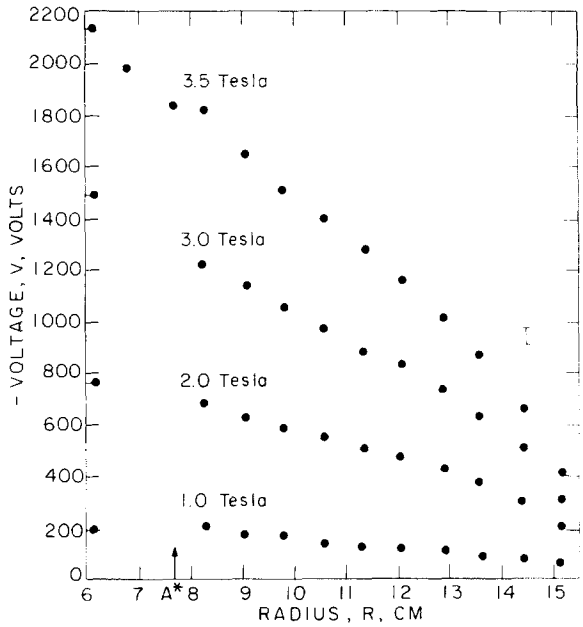

FIG. 4. Experimental voltage profiles in the disk for the uniform reference plasma (no blades).

B. Wake nonuniformities experiments

Well characterized nonuniformities are produced by the insertion of different numbers of equally spaced blades along the flow, extending from the center of the generator stagnation region to the sonic point ($r^* = 7.7$ cm). The blades are 1.0 mm thickness stainless steel with a trailing edge of 0.33 mm.

A set of experiments was performed for 6, 12, and 24 blades, and the wakes can be seen in Fig. 5.

The root mean square deviation of the conductivity, due to the presence of wakes is given in Fig. 6 as calculated (see Sec. IIIB) for the different configurations.

Figure 7 shows the calculated radial evolution of the normalized minimum velocity and minimum conductivity defect and wake width. The measured foot print of the wakes on the wall is also indicated and is found to

FIG. 5. Plasma luminosity photograph for the 24 blades case at $B = 3.5$ T, $3.5 < \beta < 7.0$.

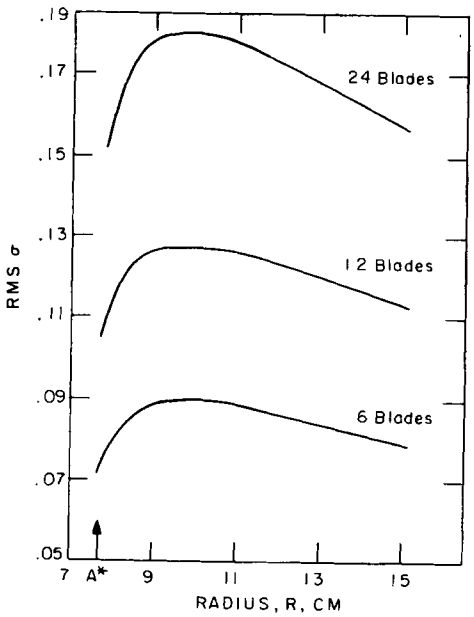

FIG. 6. Root mean square deviation of the conductivity, normalized to $\langle\sigma\rangle$, in the disk for all blade configurations.

agree with the calculated values.

Figure 8 shows the calculated normalized conductivity defect across the wake for three different radial locations.

Theoretical details are given in Sec. IIIB.

Figures 9, 10, and 11 show the measured and predicted open circuit voltage as a function of the radius for magnetic field intensities of 3.5, 3.0, and 2.0 T, respectively, for different blade configurations. The results exhibit the effect of the nonuniformities on the performance of the generator. For example, the average electric field ratio, as compared with its uniform value, is 0.77 in the six blade case at 3.5 T, while it drops to 0.46 in the 24 blade case. A complete analysis and comparison between the experimental and theoretical results are discussed in Sec. IV.

Figures 12 and 13 show the effective Hall coefficient

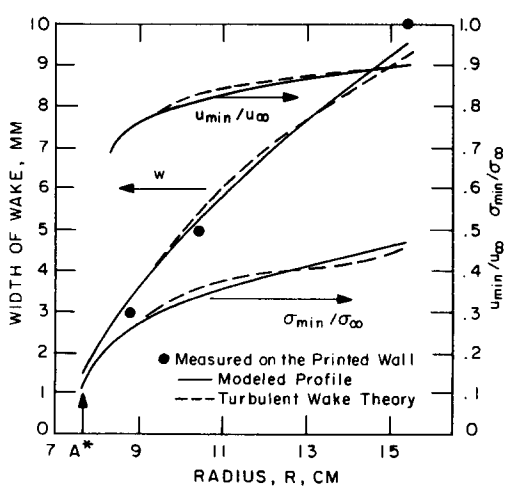

FIG. 7. Minimum conductivity and velocity deficit ratio and width of the wake along the disk.

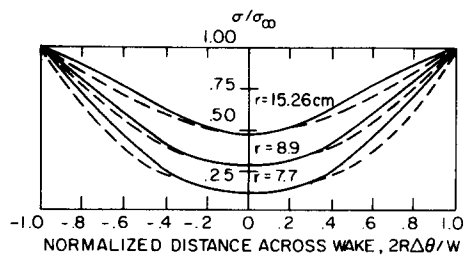

FIG. 8. Normalized conductivity ratio across the wake at three different radii, _____modeled profile---turbulent wake theory.

along the disk for all blade configurations at 3.5 and 2.0 T, respectively. The upper and lower curves on the top represent the ideal "region" for the Hall coefficient for the uniform reference (no blades) case, where the run-to-run pressure variation, as shown in Fig. 3, was taken into consideration in the calculations: $\beta=\beta_c(P_c/P_m)$, where β_c and P_c are the calculated Hall coefficient and the static pressure, respectively, which were obtained from the one-dimensional model; and P_m represents the measured static pressure.

The measured effective Hall coefficient is within the ideal region and in the last portion of the channel reaches a value of 7.2 at $B=3.5$ T.

Figure 14 shows the electric field ratio as a function of the ideal Hall coefficient at $r=11.40$ cm close to the middle of the channel.

Figures 15 and 16 show the complete set of experimental and theoretical relations between the effective and the ideal Hall coefficient at the entrance, middle, and exit of the test section for different blade configurations.

III. THEORETICAL MODELING OF NONUNIFORMITIES EFFECTS

An engineering model based on a generalization of Rosa's layer model is presented, and its validity is

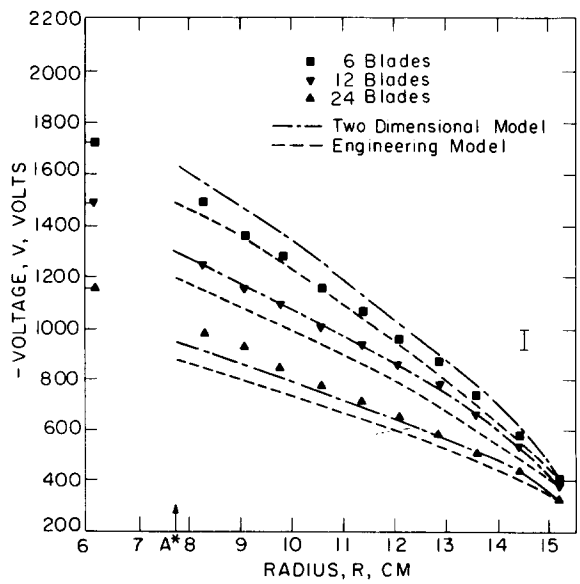

FIG. 9. Experimental and theoretical voltage profile in the disk for all blade configurations at $B=3.5$ T, $3.5<\beta<7.0$.

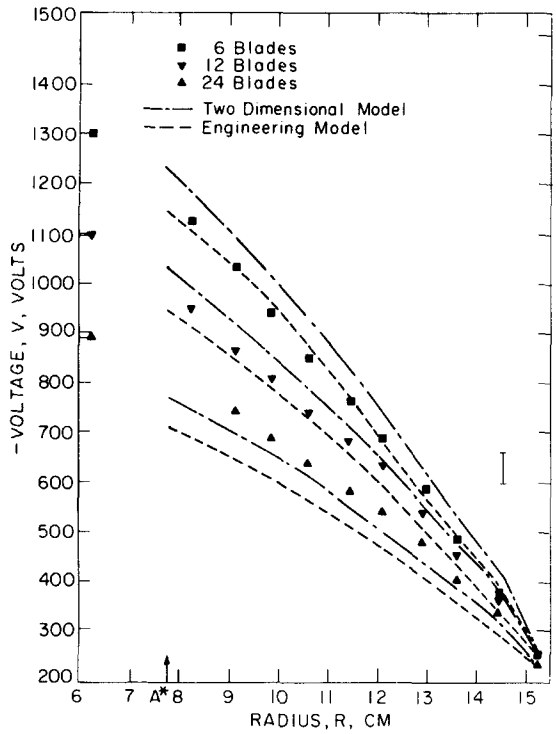

FIG. 10. Experimental and theoretical voltage profile in the disk for all blade configurations at $B = 3.0$ T, $2.9 < \beta < 6.0$.

checked by detailed two-dimensional electrodynamic calculations. Comparison with the experimental results is presented in Sec. IV.

A. The engineering model

Rosa's well known solution for the average Ohm's law in a constant-density plasma with a parallel layer structure[1] can be generalized to the case where σ, β, and radial velocity have two-dimensional variations with the variation being strong in a preferred direction. In the setting of the magnetohydrodynamic device with disk geometry the strong variations are across the wake in the azimuthal direction as compared with the secondary variations along the radial direction. Therefore, for narrow radial wakes, one can assume, approximately, that

$$E_r = E_r(r), \quad J_\theta = J_\theta(r), \quad \text{and} \quad \langle E_\theta \rangle = 0, \tag{2}$$

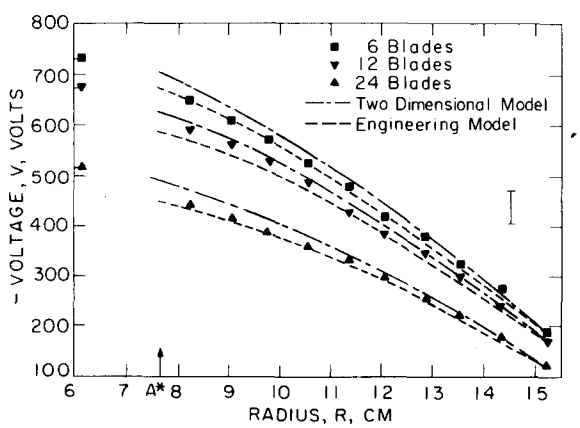

FIG. 11. Experimental and theoretical voltage profile in the disk for all blade configurations at $B = 2.0$ T, $1.90 < \beta < 4.26$.

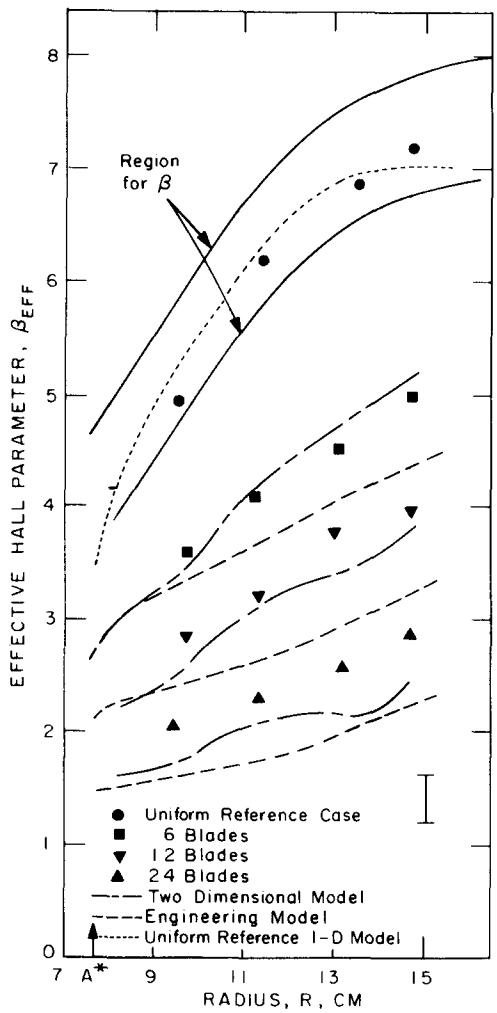

FIG. 12. Measured and calculated Hall parameter, for all blade configurations, in the disk for $B = 3.5$ T, $3.5 < \beta < 7.0$.

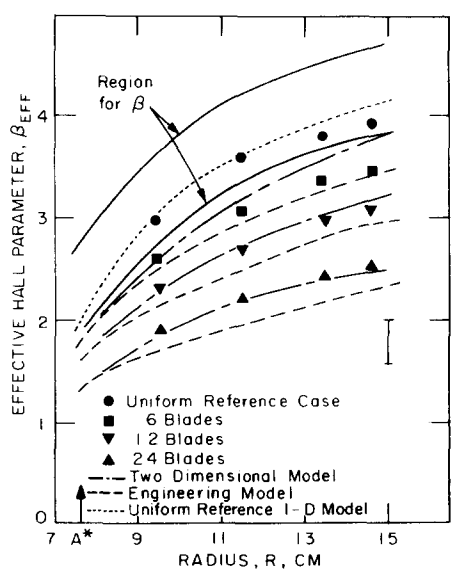

FIG. 13. Measured and calculated Hall parameter, for all blade configurations in the disk for $B = 2.0$ T, $1.90 < \beta < 4.26$.

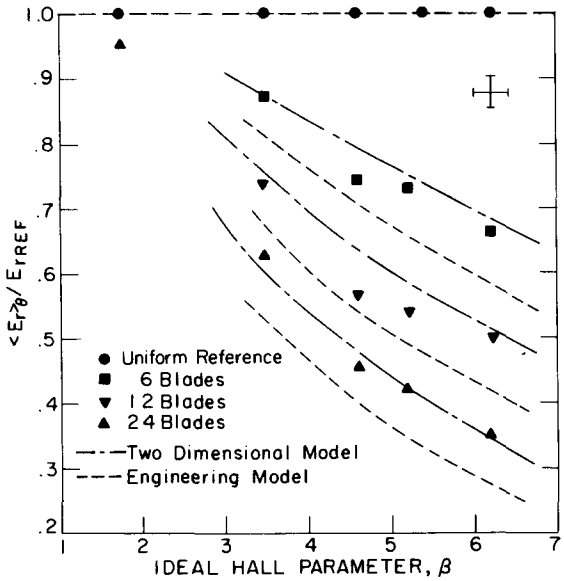

FIG. 14. Comparison of the theoretical and experimental normalized average radial electric field with the ideal Hall parameter for all blade configurations at $R = 11.40$ cm.

where E_r, E_θ and J_r, J_θ are the radial and azimuthal electric field and current density, respectively. Ohm's law can be averaged in the azimuthal direction, with the result (for the azimuthal velocity, $u_\theta \equiv 0$)

$$\langle J_r\rangle_\theta + \langle\beta\rangle_\theta J_\theta = \langle\sigma\rangle_\theta E_r\,, \tag{3}$$

$$\langle(1+\beta^2)/\sigma\rangle_\theta J_\theta = -\langle u_r\rangle_\theta B + \langle\beta\rangle_\theta E_r\,, \tag{4}$$

where u_r is the radial velocity and all averages can still depend on r. Using current conservation

$$\langle J_r\rangle_\theta = I/2\pi r h(r)\,, \tag{5}$$

where I is the total current and $h(r)$ is the generator height, one can solve for the radial field E_r

$$E_r = \frac{\langle(1+\beta^2)/\sigma\rangle_\theta (I/2\pi r h) - \langle\beta\rangle_\theta\langle u_r\rangle_\theta B}{G(r)}\,. \tag{6}$$

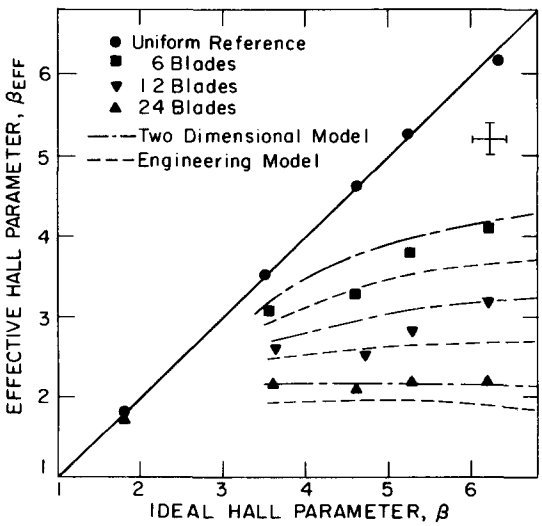

FIG. 15. Comparison of the measured and calculated effective Hall parameter with the ideal for all blade configurations at $R = 11.40$ cm.

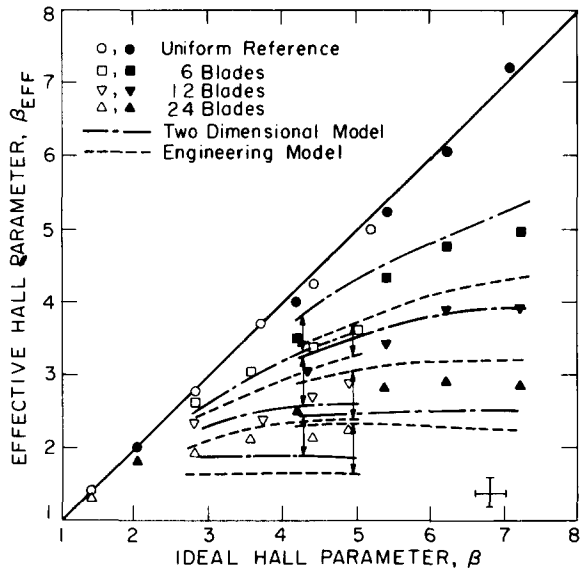

FIG. 16. Comparison of the measured and calculated effective Hall parameter with the ideal for all blade configurations at two different locations: □, ▽, △, $R = 9.6$ cm; ■, ▼, ▲, $R = 14.60$ cm.

Here, $G(r)$ is Rosa's nonuniformity factor

$$G(r) = \langle\sigma\rangle_\theta\langle(1+\beta^2)/\sigma\rangle_\theta - \langle\beta\rangle_\theta^2 \geq 1. \tag{7}$$

Integrating from inlet to outlet gives the generator load line

$$V = \int_{r_1}^{r_2} \frac{\langle\beta\rangle_\theta\langle u_r\rangle_\theta B}{G(r)}\,dr - I\int_{r_1}^{r_2} \frac{\langle(1+\beta^2)/\sigma\rangle_\theta dr}{2\pi r h(G)}\,, \tag{8}$$

from which the open circuit voltage and the short circuit current follow immediately.

For our experiment in the open circuit case one gets

$$\beta_{eff}(r) = \langle\beta\rangle_\theta / G(r)\,, \tag{9}$$

and

$$V = \int_{r_1}^{r_2} \frac{\langle\beta\rangle_\theta\langle u_r\rangle_\theta B}{G(r)}\,dr\,. \tag{10}$$

B. Detailed two-dimensional electrodynamic calculations

In order to explore the limitations of the engineering model and obtain a more detailed comparison with the experimental results, two-dimensional electrodynamic calculations were carried out for the disk geometry corresponding to the experimental channel.

The conductivity, velocity, and ideal Hall coefficient were obtained using the one-dimensional calculations for the uniform reference case which account for the effects of both the ordinary hydrodynamic forces and the magnetohydrodynamic interaction in the open circuit mode.

Conductivity and velocity wakes were then imposed in the form of modeled profiles which are consistent with the following simplified treatment of turbulent wake formation: The Schlichting[11] model for the spread of two-dimensional turbulent velocity-defect wakes was adopted, using as initial values the results of thermal and velocity boundary layer calculations[12] over the blade

surfaces. The enthalpy defect profiles were related to the velocity defect profiles using an empirical relation due to Reichardt.[11]

Assuming Saha equilibrium for the electrons, the conductivity defect was then obtained. Figures 7 and 8 show the evolution of the intensity and width of the modeled wake as compared with the treatment of wake formation. The effect of the Hall parameter defect in the wake is negligible for this case due to its mild dependence on temperature defect and the narrowness of the wake ($\langle\beta\rangle_\theta = 0$).

The differential equation governing the electric potential

$$\frac{\partial}{\partial r}\left[rh\hat{\sigma}\left(-\frac{\partial\phi}{\partial r}+\frac{\beta}{r}\frac{\partial\phi}{\partial\theta}\right)\right]+\frac{\partial}{\partial\theta}\left[\hat{\sigma}h\left(\frac{1}{r}\frac{\partial\phi}{\partial\theta}-\beta\frac{\partial\phi}{\partial r}\right)\right]$$
$$=B\left(\frac{\partial}{\partial r}[rh\hat{\sigma}(u_\theta+\beta u_r)]+\frac{\partial}{\partial\theta}[h\hat{\sigma}(-u_r+\beta u_\theta)]\right), \qquad (11)$$

where $\hat{\sigma}=\sigma/(1+\beta^2)$ is solved over a basic period subject to periodic boundary conditions in the azimuthal direction and prescribed potentials at the inner and outer radii (electrodes).

The over-relaxation method was used for the numerical solution over a variable grid structure in which to capture the effect of the narrowness of the wakes and adjust the refinement of the spacing in places of sharp gradients.

IV. ANALYSIS AND COMPARISON BETWEEN EXPERIMENTAL AND THEORETICAL RESULTS

The comparisons between the experimental and theoretical results for the two models are shown in Figs. 9–18. The theoretical electric potential is normalized in each case so as to have the corresponding measured experimental values at the exit of the generator. The choice of the exit point for normalization is, of course, arbitrary, but it was chosen to display the largest possible deviations between the experimental and theoretical results at the inlet (Figs. 9, 10, and 11).

The wake profiles were imposed according to the procedure described in Sec. IIIB. All cases were subjected to the same type of wake intensity and evolution shown in Figs. 7 and 8. It should be noted that, although the intensity and evolution of the wake are the same for all cases, the weighted root mean square deviations (rms) of the conductivity and velocity are different for different numbers of blades due to different volume fractions occupied by the background plasma in each case.

Inspection of the results reveals several important points.

(1) The theoretical open circuit voltages (Figs. 9, 10, and 11) obtained from the engineering and two-dimensional models are in very good agreement with experimental results.

(2) The engineering model slightly overpredicts the degrading effects of the open circuit voltage as compared with the two-dimensional calculations. The differences in predictions ranged from 7.7% at $B=2.0$ T to 13% at $B=3.5$ T can be accounted for in part by the infinite plasma approximation in the engineering model and in part by the streamwise increase of the layer thickness.

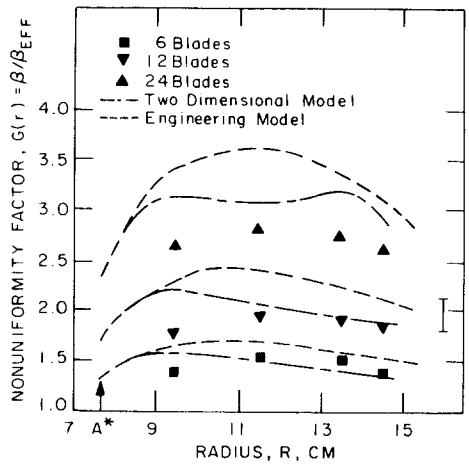

FIG. 17. Experimental and theoretical nonuniformity factor profile in the disk for $B=3.5$ T, $3.5<\beta<7.0$.

(3) The distortion of the equipotential lines across the wake [Figs. 18(a) and 18(b)] is due to the strong deficit of conductivity, which generates a local highly resistive medium for the current at the location of steep conductivity gradients.[7]

(4) Figures 14, 15, and 16 show the dependence of the normalized average electric field and the effective Hall coefficient at three different locations in the channel, on the ideal Hall parameter, and the rms σ. The discontinuity in the curves that are shown in Fig. 16 for $3.9 \leq \beta \leq 4.6$ in each blade configuration is due to differences in the wake evolution (i.e., differences in rms σ) at the two locations $r=9.6$ cm and $r=14.6$ cm.

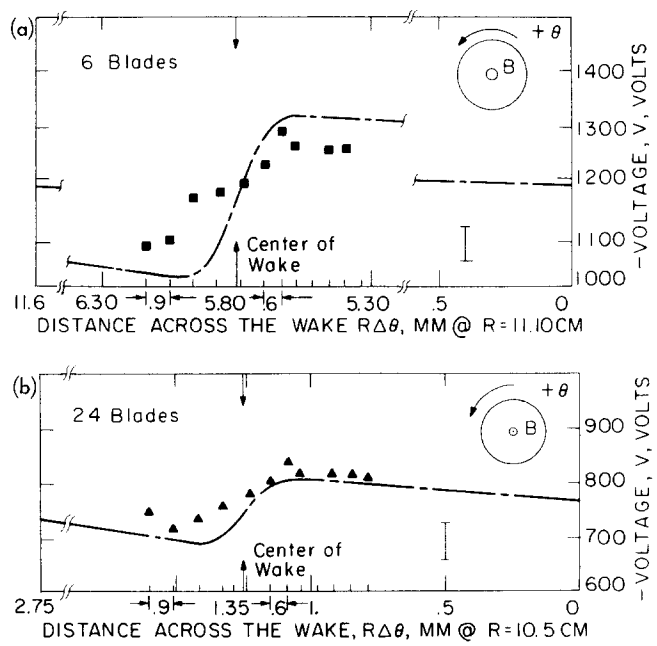

FIG. 18. Experimental and theoretical voltage profiles across the wake for $B=3.5$ T, $3.5<\beta<7.0$. (a) Six blade case; (b) 24 blade case.

(5) For a fixed rms σ (fixed number of blades) the degrading effects on the performance increase as the Hall coefficient increases (higher magnetic fields) (Figs. 12, 13, 14, 15, and 16).

(6) For a fixed magnetic field intensity (same range of Hall coefficient) the degrading effects increase as rms σ increases (larger number of blades) (Figs. 12, 13, 14, 15, and 16).

(7) The trend of the effective Hall coefficient (Figs. 14 and 15) is in agreement with that of a "strongly unsymmetric plasma," (Ref. 5, Figs. 5 and 7), in the sense that the most conductive regions occupy a large portion of the plasma leaving the remainder to low-conductivity regions. The degradation is less severe here than in the case of "symmetric" plasmas, in which the effective Hall coefficient β_{eff}, saturates at high ideal β. This latter effect is well known in unstable nonequilibrium plasmas.

The degrading trend of the effective Hall coefficient (Figs. 12, 13, 15, and 16) can be seen from a further analysis of the formulas for β_{eff} and $G(r)$ in Eqs. (7) and (9):

If $\beta(r)$ is fixed across the wake, one gets

$$G(r)=1+\alpha_N(1+\beta^2), \tag{12}$$

and

$$\beta_{eff}=\beta/[1+\alpha_N(1+\beta^2)], \tag{13}$$

where $\alpha_N=\langle\sigma\rangle_\theta\langle 1/\sigma\rangle_\theta-1$, is termed the nonuniformity factor.

An examination of Eqs. (12) and (13) reveals that there are two factors controlling the degradation of the effective Hall coefficient:

(i) the level of nonuniformities as measured by the rms σ, which depends on the distance between blades, intensity and width of the wake; and

(ii) the value of the ideal Hall coefficient, β.

Figure 17 shows the evolution of Rosa's nonuniformity factor, $G(r)$, with experimental comparison for $B=3.5$ T. The corresponding influence of the $G(r)$ factor on the effective Hall coefficient is in agreement with the trend of $G(r)=\beta/\beta_{eff}$.

An analogy can be drawn about the $G(r)$ factor in the disk and linear magnetohydrodynamic devices when the distances in the azimuthal and radial directions are equated to distances in the transverse, y, and axial directions, respectively. In this analogy, the plasma properties inside the boundary layers of the corresponding linear generator are equivalent to the same properties inside one wake in the disk.

V. CONCLUSIONS

The experimental and theoretical results of the two-dimensional nonuniformities, with strong variations in the plasma properties in the direction normal to the magnetic field and the flow, confirm the strong degradation of the effective Hall coefficient when β and the rms σ of these nonuniformities are high. The experimental results are in good agreement with predictions from two theoretical models derived from a two-dimensional analysis and a simplified engineering model. These experiments validate the analytical studies and support the use of the theoretical layer models used to describe the effect of boundary layers on the performance of linear magnetohydrodynamic devices.

ACKNOWLEDGMENTS

The authors wish to acknowledge the advice of Professor Manuel Martinez-Sanchez, Dr. William Loubsky, and Dr. J. Derek Teare and the assistance of Mr. Walter Littlewood.

This work was sponsored by the United States Department of Energy under contract DE-AC01-79FT15518.

[1]R. J. Rosa, Phys. Fluids **5**, 1081 (1962).
[2]A. M. Dykhne, Zh. Eksp. Teor. Fiz. **59**, 641 (1970) [Sov. Phys.–JETP **32**, 348 (1971)].
[3]I. U. Emets, A. P. Rasheheskin, V. F. Reagtsov, and A. K. Shidlovskiy, in *Proceedings of the Sixth International Conference on Magnetohydrodynamic Electrical Power Generation* (National Technical Information Service, Springfield, Va., 1975), Vol. 4, p. 203.
[4]J. F. Louis, Phys. Fluids **10**, 2062 (1967).
[5]S. E. Shamma, M. Martinez-Sanchez, and J. F. Louis, Phys. Fluids **21**, 773 (1978).
[6]S. J. Schneider and J. F. Louis, in *Proceedings of the 14th Symposium on Engineering Aspects of Magnetohydrodynamic* (The University of Tennessee Space Institute, Tullahoma, Tenn, 1974), p. V.2.1.
[7]S. D. Dvore, M. Martinez-Sanchez, and S. E. Shamma, in *Proceedings of the 17th Symposiumon Engineering Aspects of Magnetohydrodynamic* (High Temperature Gasdynamics Laboratory, Stanford University, Stanford, California, 1978), p. B.2.1.
[8]W. J. Loubsky, J. K. Lytle, J. D. Teare, and J. F. Louis, in *Proceedings of the 11th International Symposium on Shock Tubes and Waves* (University of Washington Press, Seattle, Wash., 1977), p. 498.
[9]R. A. Svebla and J. McBride, NASA TN D-7056 (1973).
[10]J. K. Lytle, W. Loubsky, M. Rosenbaum, and J. F. Louis, in *Proceedings of the 18th Symposium on Engineering Aspects of Magnetohydrodynamics* (Office of Magnetohydrodynamic and Energy Research, Montana State University, Butte, Montana, 1979), p. D-2.5.1.
[11]H. Schlichting, *Boundary Layer Theory* (McGraw-Hill, New York, 1960).
[12]W. D. McNally, NASA TN D-5681 (1970).